Broadband self-pulsating fiber laser based on soliton self-frequency shift and regenerative self-phase modulation

Thibault North and Martin Rochette*

Department of Electrical and Computer Engineering, McGill University, Montréal, Québec, H3A 2A7, Canada
**Corresponding author: martin.rochette@mcgill.ca*

Received April 2, 2012; revised May 11, 2012; accepted May 16, 2012;
posted May 16, 2012 (Doc. ID 165872); published July 4, 2012

We demonstrate experimentally and numerically the operation of a self-pulsating fiber laser based on the cascaded effects of soliton self-frequency shift and self-phase modulation spectral broadening. The combination of those two effects triggers and sustains the propagation of picosecond pulses in the cavity. At one of the outputs, the laser emits a supercontinuum with spectral width in excess of 150 nm at the repetition rate of 95 kHz. © 2012 Optical Society of America

OCIS codes: 060.3510, 140.0140, 140.3510, 190.4370, 320.5390.

Pulsed fiber lasers have been investigated in the past few years for their applications in industrial processes, instrumentation, and optical telecommunications. Based on a technique suggested in [1], we have presented a self-pulsating laser source based on cascaded optical regeneration working at a wavelength of 1550 nm [2,3]. With a different laser architecture, this regenerative approach was also theoretically expected to operate at a wavelength of 1060 nm [4]. In contrast with traditional mode-locked lasers that take advantage of mechanisms such as nonlinear polarization rotation and saturable absorption [5], a regenerative source induces and sustains the oscillation of one or several pulses, called eigenpulses, that are altered and regenerated in every cavity round trip. With external dispersion compensation, it was shown that both sources generate subpicosecond pulses. Such kinds of pulses enable the generation of supercontinua, generally by their propagation in a nonlinear medium [6] and sometimes with an additional nested cavity, for example, used for the slicing of an octave-spanning supercontinuum [7]. With pump powers higher by an order of magnitude in comparison with the methods described above, it was also shown that supercontinua could be generated in continuous-wave laser cavities [8] and with self-pulsating lasers producing pulses of several kilowatts of peak power in the Q-switched regime [9,10].

In this letter, we experimentally and numerically demonstrate a regenerative source based on the cascaded effects of soliton self-frequency shift (SSFS) as well as self-phase modulation (SPM) spectral broadening [11,12]. Together, these two mechanisms provide a stable pulsed equilibrium leading to a set of picosecond pulses and supercontinuum generation from pico- and subpicosecond pulses. To the best of our knowledge, this is the first demonstration of the use of SSFS as a condition for pulse generation, as well as the first demonstration of a self-pulsating source that produces a supercontinuum from nonlinear effects in its own cavity. The presented device is simple to implement and provides a supercontinuum without the need for an external mode-locked laser.

Figure 1(a) shows a schematic of the cavity used in the experiment. It comprises a loop divided in two halves with distinctive nonlinear functions.

In the first half of the cavity, the first highly nonlinear fiber (HNLF) HNLF_1 of waveguide nonlinear coefficient $\gamma = 11.5\ \mathrm{W^{-1}\,km^{-1}}$ and chromatic dispersion coefficient $D_1 = -0.71\ \mathrm{ps\,nm^{-1}\,km^{-1}}$ induces SPM spectral broadening to propagating pulses. To complete the SPM regeneration process with offset filtering, a fiber Bragg grating (FBG) is used in tandem with an optical circulator to provide bandpass filtering over a bandwidth of 5.0 nm centered at $\lambda_1 = 1544.0$ nm. The first half of the cavity is completed with chromatic dispersion compensation of HNLF_1 by using 42 m of standard single-mode fiber.

In the second half of the cavity, the mechanism of pulse selection is SSFS followed by filtering. Fiber HNLF_2 has $\gamma = 11.5\ \mathrm{W^{-1}\,km^{-1}}$ and anomalous dispersion with $D_2 = 2.09\ \mathrm{ps\,nm^{-1}\,km^{-1}}$. The nonlinear fiber is followed by a tunable bandpass filter (BPF) with 6.2 nm of bandwidth centered at $\lambda_2 = 1550.5$ nm to select pulses that have experienced a specific amount of wavelength shift. In each half, various couplers $C_{1\text{–}4}$ are used for

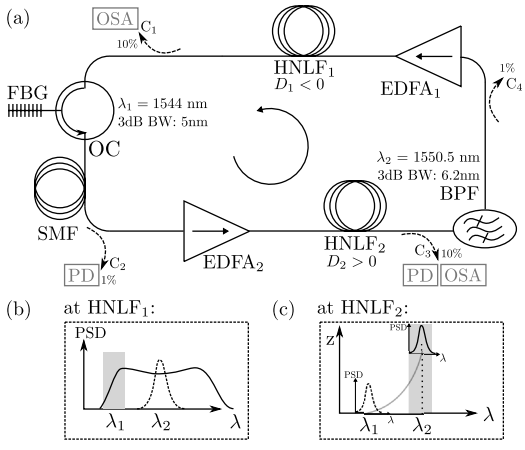

Fig. 1. (a) Schematic of the experimental setup. (b), (c) Spectra representing the pulse before (dashed line) and after (solid line) propagation in each HNLF. OC, optical circulator; OSA, optical spectrum analyzer; HNLF, highly nonlinear fiber; EDFA, erbium-doped fiber amplifier; BPF, bandpass filter; FBG, fiber Bragg grating; BW, bandwidth; PD, photodiode; SMF, single-mode fiber; PSD, power spectral density.

monitoring purposes. Figures 1(b) and 1(c) illustrate in the frequency domain the result of the propagation of pulses in each half of the cavity. Insertion losses are 1.7 dB for $HNLF_1$, 3.3 dB for the grating and optical circulator combination, 1.2 dB for $HNLF_2$, and 9.9 dB for the tunable BPF. Each coupler has an insertion loss of ~0.5 dB in addition to the losses expected from the coupling coefficient.

The pulses propagating in the cavity are monitored spectrally using optical spectrum analyzers (OSAs) connected to 10% tap couplers $C_{1,3}$ and are also monitored in time using a photodiode (PD) followed by an oscilloscope at the output of 1% tap coupler C_2. The source self-starts from the amplified spontaneous emission (ASE) of both erbium-doped fiber amplifiers (EDFAs). The gain is initially set at 11.6 dB for $EDFA_1$ and 16.2 dB for $EDFA_2$. Figures 2(a) and 2(b) show the spectra observed at outputs C_1, C_2, and C_3, while Figs. 2(c) and 2(d) show oscilloscope traces of the laser output as measured from C_2 and C_3 with the PD. The trace in Fig. 2(c) shows that the laser provides a burst of power at every 10.5 μs. The trace in Fig. 2(d) shows that this burst is made up of a collection of short pulses in cascade. In inset Fig. 2(e), picosecond pulses are observed after the SPM regeneration process.

The supercontinuum observed at output C_3 originates from pulses that have experienced SSFS in $HNLF_2$, which is a required condition for a pulsed regime. It also appears from output C_1 that the pump pulses in $HNLF_1$ provide a Raman gain with a 13.2 THz offset with respect to the pump and a resulting ASE centered at 1664 nm. The absence of power at a wavelength of ~1450 nm excludes the contribution of a degenerate four-wave mixing process at the pump. It was also observed that additional bursts of pulses similar to those shown in Fig. 2(d) are created and sustained in the cavity when increasing the EDFAs gain.

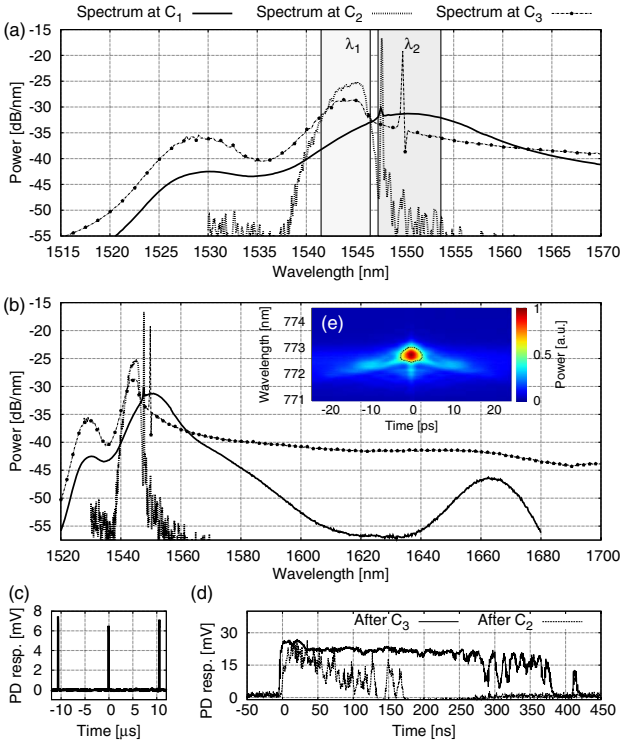

Fig. 2. (Color online) (a), (b) Spectra from outputs C_1, C_2, and C_3; (c) observed from C_2, oscilloscope trace showing the repetition rate and burst structure of the output signal; (d) observed from C_2 and C_3, oscilloscope trace zooming on one burst and revealing a structure that comprises several pulses. Inset (e) frequency-resolved optical gating spectrogram at C_2.

The circulation of pulses in the cavity was simulated and predicts self-pulsation via single-pulse operation, and the observed supercontinuum generation at higher levels of power in the presence of multiple pulses. The propagation in both HNLFs was modeled using a split-step Fourier method including the effects of the nonlinearity, the second- and third-order dispersion terms, self-steepening, and Raman scattering. Filtering was modeled with bandpass filters, and the EDFAs were modeled as perfect amplifiers with a saturable gain. To start the source, both white noise and Gaussian pulses used as a seed led to similar results. Figures 3(a) and 3(b) illustrate solitons after $HNLF_2$ for the fiftieth cavity round trip. In the frequency domain, Fig. 3(c) provides the spectra before and after propagation in $HNLF_2$, in agreement with the experimental result of Fig. 2(b). Because of the filtering at λ_1, pulses that are entering $HNLF_2$ have a full width at half maximum (FWHM) duration of ~1 ps but with a peak power of ~20 W, which corresponds to a higher order soliton of $N \cong 5.5$. Hence, we observe soliton fission during the beginning of propagation in $HNLF_2$ [13]. New solitons of various FWHM duration and peak power copropagate in the HNLF, with a group-velocity relative to their central wavelength, and an acceleration owing to the SSFS induced by the Raman effect.

Figure 4 illustrates that soliton fission occurs within the first 20 m of propagation, leading to fundamental solitons. The slope of their trajectories is related to their group-velocity dispersion, and powerful pulses slow down as a result of intrapulse Raman scattering. This figure also illustrates that the accumulated delay of these solitons is responsible for the long burst of pulses experimentally observed in Fig. 2(d).

The wide spectrum of Figs. 2(b) and 3(c) result from the propagation of several subpicosecond pulses in $HNLF_2$, which experience an amount of SSFS that

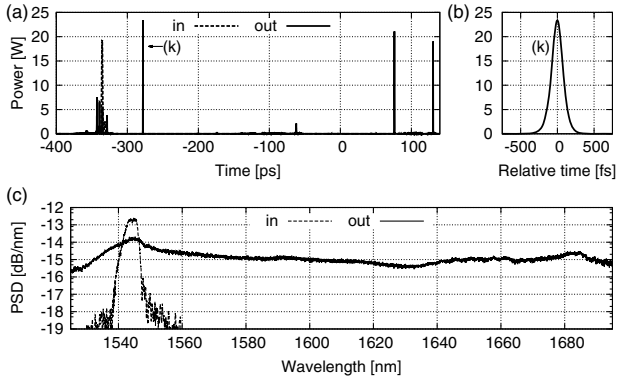

Fig. 3. Numerical simulations for the setup of Fig. 1. (a) Fundamental solitons after $HNLF_2$. (b) Zoom on the output soliton (k). (c) Spectrum obtained by an averaging of 50 round trips of the cavity, starting at round trip 10. The dashed and solid curves correspond to the input and the output of $HNLF_2$, respectively.

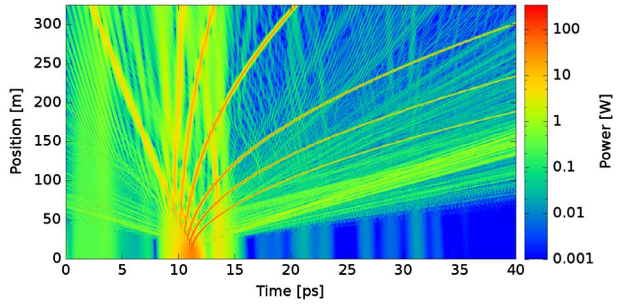

Fig. 4. (Color online) Soliton fission in the time domain and propagation of the resulting fundamental solitons in the first 300 m of $HNLF_2$.

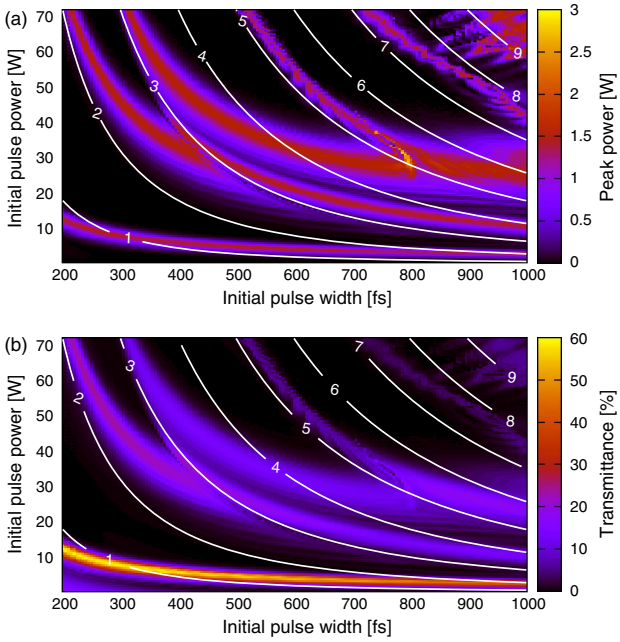

Fig. 5. (Color online) Pulses with an initial temporal width and peak power are launched in $HNLF_2$. (top) Their final peak power is represented after filtering at the BPF. (bottom) The transmittance at the filter is shown. For reference, solid lines indicate the corresponding soliton order.

depends on their own temporal width and peak power. Because the amount of SSFS is related to $1/t_{\mathrm{fwhm}}^4$ [11], only solitons with an adequate FWHM are selected by the BPF and will be sustained by the cavity for the next round trip. Figure 5(a) shows the peak power of pulses launched in $HNLF_2$ after filtering at the BPF, and Fig. 5(b) provides the associated transmittance at this BPF. Another pulse selection is performed at the regenerator, and the bandwidth of the FBG gives a first limit on the pulse temporal width. The observed pulse of Fig. 2(e) is about three times longer than expected by simulation and has pedestals because of the presence of multiple pulses in the cavity.

We have demonstrated a self-pulsating ring laser that cascades the effects of SSFS and SPM broadening followed by offset filtering. A burst of pulses is generated once per cavity round trip, yielding to a 150 nm flat supercontinuum.

The authors are thankful to Dr. Pierre Galarneau for his constructive comments and the National Optics Institute (INO), Quebec City, for their financial support.

References

1. S. Pitois, C. Finot, and L. Provost, Opt. Lett. **32**, 3263 (2007).
2. M. Rochette, L. R. Chen, K. Sun, and J. Hernandez-Cordero, IEEE Photon. Technol. Lett. **20**, 1497 (2008).
3. K. Sun, M. Rochette, and L. R. Chen, Opt. Express **17**, 10419 (2009).
4. S. Pitois, C. Finot, L. Provost, and D. Richardson, J. Opt. Soc. Am. B **25**, 1537 (2008).
5. L. Nelson, D. Jones, K. Tamura, H. Haus, and E. Ippen, Appl. Phys. B **65**, 277 (1997).
6. J. Price, K. Furusawa, T. Monro, L. Lefort, and D. Richardson, J. Opt. Soc. Am. B **19**, 1286 (2002).
7. D. Kielpinski, M. Pullen, J. Canning, M. Stevenson, P. Westbrook, and K. Feder, Opt. Express **17**, 20833 (2009).
8. M. Prabhu, N. Kim, and K. Ueda, Jpn. J. Appl. Phys. **39**, L291 (2000).
9. A. Martinez-Rios, I. Torres-Gómez, G. Anzueto-Sanchez, and R. Selvas-Aguilar, Opt. Commun. **281**, 663 (2008).
10. S. Chernikov, Y. Zhu, J. Taylor, and V. Gapontsev, Opt. Lett. **22**, 298 (1997).
11. J. Gordon, Opt. Lett. **11**, 662 (1986).
12. P. Mamyshev, in *Proceedings of the 24th European Conference on Optical Communication*, (IEEE, 1998), Vol. 1, pp. 475–476.
13. K. Tai, A. Hasegawa, and N. Bekki, Opt. Lett. **13**, 392 (1988).